Quantitative Identification of Multiple Cracks in a Rotor Utilizing Wavelet Finite Element Method

Bing Li[1,2] **and Hongbo Dong**[1]

Abstract: Different from single crack identification method, the number of cracks should be firstly identified, and then the location and depth of each crack can be predicted for multiple cracks identification technology. This paper presents a multiple crack identification algorithm for rotor using wavelet finite element method. Firstly, the changes in natural frequency of a structure with various crack locations and depths are accurately obtained by means of wavelet finite element method; and then the damage coefficient method is used to determine the number and region of cracks. Finally, by finding the points of intersection of three frequency contour lines in the small region containing crack, the crack location and depth can be predicted. Multiple cracks diagnostic examples in rotor under two working conditions have shown the effectiveness of current method: with a maximum error of crack location identification 0.6% and of crack depth identification 0.7%.

Keywords: Multiple cracks; Rotor; Identification; Wavelet finite element method

1 Introduction

Rotating machines are extensively used in diverse engineering applications, such as power station, marine propulsion systems, aircraft engines, etc. The operating speed, power, and load of rotating machinery will increase if weight and dimensional tolerance decrease for operation at higher mechanical efficiency. Consequently, many practical rotor dynamic systems contained rotor elements are highly susceptible to transverse cracks due to fatigue [Green and Casey (2005)]. A crack not detected in time can result in catastrophic failure and cause injuries and severe damage to machinery. Many investigators have studied the crack identification problems in structures [Morassi (2001); Lele and Maiti (2002); Gasch (1993); Dimarogonas (1996); Salawu (1997)]. Morassi proposed a detect method for shaft

---

[1] State Key Laboratory for Manufacturing System, Xi'an Jiaotong University, Xi'an 710072, China
[2] Corresponding author: Tel.: +86-29-82663689; fax: +86-29-82663689; E-mail address: bli@mail.xjtu.edu.cn (B. Li)

with an open crack, which is based on the changes in a pair of natural frequencies and closed-form solutions of the structures [Morassi (2001)]. Lele and Maiti investigated crack identification techniques by using eight-node iso-parametric elements to make an efficient calculation for single crack identification in structures [Lele and Maiti (2002)]. Sekhar proposed a model-based method which replaced the fault-induced change of the shaft by equivalent loads in the finite element method (FEM) [Sekhar (2004)]. Anjan using an adaptive *h*-version FEM for structure damage detection in order to control the discretization error because the traditional finite elements are impotent to describe the singular behavior of cracks and numerous elements are needed for numerical computation [Anjan and Talukdar (2004)]. Gasch [Gasch (1993)], Dimarogonas [Dimarogonas (1996)], Salawu [Salawu (1997)], and Sekhar [Sekhar (2011)] reviewed crack identification methods based on the dynamic behavior changes. And many new methods have also been introduced at the 7th vibration engineering meeting in 2011 (VETOMAC 2011). However, most methods concerning crack identification deal with single crack, the case of multiple cracks has not received the same degree of attention.

In the structural damage, there is often more than one type of crack occurring in more than one region, actually. If the damage identification is dealt blindly with the single crack detection method when the damage situation is still unknown, it will probably lead to miss report or give false information about the fault. Therefore, it is of great importance to accurately diagnose the specific location and depth of each crack. Quantitative identification of multiple cracks is much more complicated than that of single crack mainly because of the following two aspects:

The cracks will destroy the continuity of the entire structure and with the occurrence of each crack, four boundary condition equations will be introduced which will undoubtedly increase the difficulty of crack analysis;

In the multiple cracks diagnosis, the number of cracks should be firstly identified, and then the location and depth of each crack can be predicted, obviously it is more complex than the single crack diagnosis.

Some investigators have studied the quantitative identification of multiple cracks in structures in recent years [Patil and Maiti (2003); Xiang and Liang (2011); Chen, Li, Zi and He (2005); Bao and Wang (2011); He and Lu (2010); Zhang, Han and Li (2010)]. The first idea of multiple cracks identification came from the damage coefficient method present by Hu and Liang [Liang, Hu and Choy (1992); Hu and Liang (1993)]. They divided a beam containing an arbitrary number of cracks into several finite segments and each segment might contain cracks. From the energy point of view, they considered that the natural frequency of the beam had a linear correlation with the crack parameters (crack position and depth). And by means of symbolic computation method, they worked out the specific relation expression:

$\Delta\boldsymbol{\omega}/\boldsymbol{\omega} = 2\mathbf{HS}$, where $\Delta\boldsymbol{\omega}/\boldsymbol{\omega}$ is the column matrix representing the change rate of the natural frequency, matrix $\mathbf{H}$ is the influence matrix and matrix $\mathbf{S}$ is the damage coefficient matrix. The damage coefficient $\mathbf{S}$ will be obtained by solving the above equation. And if the coefficient of the unit is greater than zero, this unit would be diagnosed as a cracked unit and the magnitude of the coefficient reflected the crack depth.

Based on the damage coefficient method, Sekhar considered the difference of different crack depths and crack locations on rotor dynamic characteristics, analyzed a rotor containing two open cracks with FEM and calculated its characteristic frequency and main vibration mode [Sekhar (2008)]. Ruotolo and Surace investigated the bending vibration of bars with a random number of open cracks and proposed the smooth function method and transfer matrix method to calculate the vibration of a bar with multiple cracks and the solution agreed well with the experimental results [Ruotolo and Surace (2004)]. Moreover, Hollander [Hollander, Wunsche, Henkel and Theilig (2012)], Lee [Lee (2009)], Lin [Lin and Cheng (2008)], and Lam [Lam and Yin (2010)] also have explored the analytic and finite element methods for the multiple cracks problem.

However the analytic method is difficult to be used to calculate the dynamic behaviors for cracked structures with complex geometry. In additionally, because of the fact that the crack tip field displacement and stress have $1/\sqrt{\tau}$ singularity (τ denotes crack tip field radius in polar coordinates) and the traditional FEM piecewise polynomial cannot approximate them accurately on a local area [Kardestuncer and Norrie (1987)], a fine mesh and great amount of computational work is required when the traditional finite elements are used to describe the singular behavior of cracks. To overcome these difficulties, wavelets have been applied to finite element analysis because wavelet multiresolution theory provides a powerful mathematical tool for function approximation and multiscale representations. Since B-Spline wavelet on the interval (BSWI) has explicit expressions, which allows us to conveniently calculate the element stiffness matrix. Furthermore, B-spline wavelets have the best approximation properties among all known wavelets of a given order and wavelets on the interval have good characteristic of localization, which can overcome some numerical instability phenomena [Goswami, Chan and Chui (1995)]. Therefore, Scaling functions of BSWI at a certain scale are adopted to form the shape functions and construct wavelet-based elements. Xiang [Xiang, Zhong, Chen and He (2008)], Li [Li, Dong, Xiang, Qi and He (2011)], and Dong [Dong, Chen, Li, Qi and He (2009)] constructed wavelet-based crack elements of BSWI to build FEM models of a cracked rotor and clamped beam with a rectangular cross-section, and then identified the crack location and size by using the first three simulative frequencies of single cracked structures.

In this paper, we introduced wavelet finite element method (WFEM) to multiple cracks identification problems, and present a quantitative algorithm for the detection of each crack in rotor. Firstly, the changes in natural frequency of a structure with various crack locations and depths are accurately obtained by means of wavelet finite element method; and then the damage coefficient method is used to determine the number and region of cracks. Finally, by finding the points of intersection of three frequency contour lines in the small unit containing crack, the crack location and depth can be identified. To verify the effectiveness of the presented method, we have performed simulations in rotor with multiple cracks. The results of the multiple cracks diagnosis tests under two working condition cases are as follows: with a maximum error of crack location detection 0.6% and of crack depth detection 0.7%.

2   Theoretical basis

2.1   *The basic principle of crack identification*

The crack will introduce local flexibility to the structure which changes dynamic characteristics of the whole structure. In vibration diagnosis, structure frequency change is regarded as the basis of structure crack identification [Naniwadekar, Naik and Maiti (2008)]. Usually, the frequency-based crack detection method includes two procedures [Li, Chen and He (2005)]. The forward problem is to determine the first three natural frequencies of the cracked structure given the location and depth of the crack. The inverse problem is to determine the location and depth of the crack given the first three natural frequencies of the cracked beam.

As for a structure, its natural frequency is changed with the appearance of cracks. Let $\omega_n\,(n = 1,2,3,\ldots)$ be the nth order natural frequency, the relationship among crack location, depth and natural frequency of the beam are as follows£º

$$\omega_n = g\,(a,b)\,, \quad (n = 1,2,3,\ldots) \tag{1}$$

Where a and b are the position and depth of the crack respectively, shown in Fig. 1. The forward problem of crack identification can be viewed as to solve the natural frequency of the structure with the known function $g(a,b)$ and crack parameters a and b.

If the measured natural frequency is known, the inverse problem, that is to determine the location and depth of the cracks, can be described with the following function:

$$(a,b) = g^{-1}\,(\omega_n)\,, \quad (n = 1,2,3,\ldots) \tag{2}$$

Therefore, if the function $g^{-1}(\omega_n)$ is known, the crack location and depth can be obtained with the measured natural frequency values. The process of crack identification is showed in Fig.2. The identification procedure is briefly described as following.

- The crack on the structure is equivalent as a rotational spring and the equivalent stiffness is evaluated by linear fracture mechanics approach;

- By solving local crack stiffness matrix and adding the local crack stiffness matrix into the global stiffness matrix, the high performance wavelet-based model for cracked structure is built up;

- Solve the first three natural frequencies under different normalized crack location and depth, and then the crack detection database are obtained by means of surface-fitting techniques.

The first three measured natural frequencies through test in physical model are employed as the inputs of the inverse problem and the crack parameters can be identified by frequency contour method.

(a)   (b)
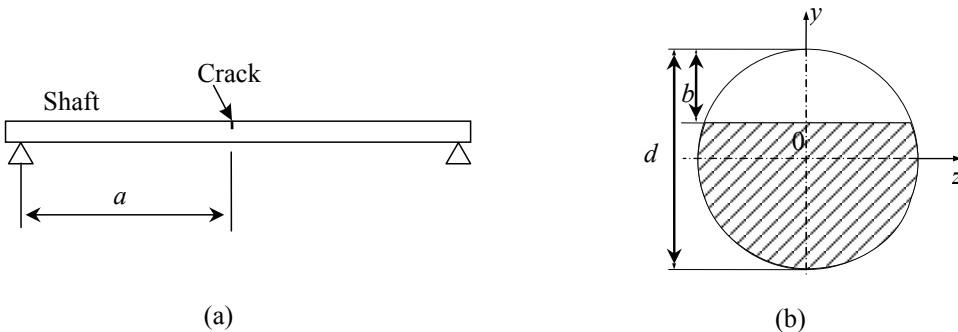
Figure 1: Crack parameters (a) Crack location (b) Crack depth.

2.2   *Forward problem: modal analysis using WFEM*

The basic idea of WFEM, which is similar to the traditional FEM, is to discretize a body into an assemble of discrete finite elements which are interconnected at the nodal points on element boundaries. The displacement field is approximated over each wavelet-based finite element, in terms of the nodal displacements. Li et al.
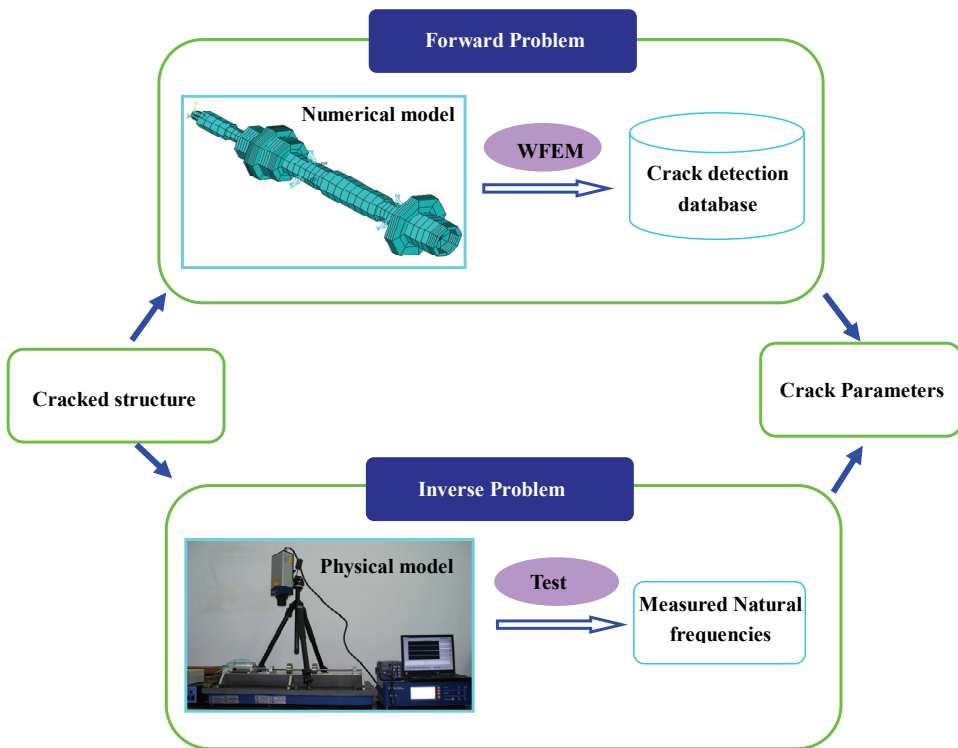
Figure 2: The process of crack identification

have constructed wavelet-based beam elements for the vibration problems of the beam with an open crack [Li, Chen and He (2005)]. Dong et al. have presented wavelet finite elements based on BSWI and applied them to the single crack identification problems [Dong, Chen, Li, Qi and He (2009)]. For completeness, the forms of the derivation of wavelet-based element equations are given here.

A shaft model with crack is shown in Fig. 1. The rotor is modeled by a Rayleigh–Euler beam considering the effects of the cross-section inertia, the elemental potential energy U^e can be written as

$$U^e = \int_0^{l_e} \frac{EI_z}{2} \left(\frac{d^2 w}{dx^2}\right)^2 dx \tag{3}$$

Where E is the Young's modulus, I_z is the moment of inertia, $w(x,t)$ is the transverse displacement, and l_e is the elemental length. The elemental kinetic energy T^e of the Rayleigh–Euler beam allowing for the rotatory inertia effect can be expressed

as

$$T^e = \int_0^{l_e} \frac{\rho A}{2} \left(\frac{\partial w}{\partial t}\right)^2 dx + \int_0^{l_e} \frac{\rho I_z}{2} \left(\frac{\partial \theta}{\partial t}\right)^2 dx \tag{4}$$

Where ρ is the density, A is the area of the cross-section, $\theta(x,t)$ is the rotation of the shaft section due to bending and can be given by $\theta = \frac{dw(x,t)}{dx} = \frac{1}{l_e}\frac{dw(\xi,t)}{d\xi}$. The layout of elemental nodes is shown in Fig. 3.
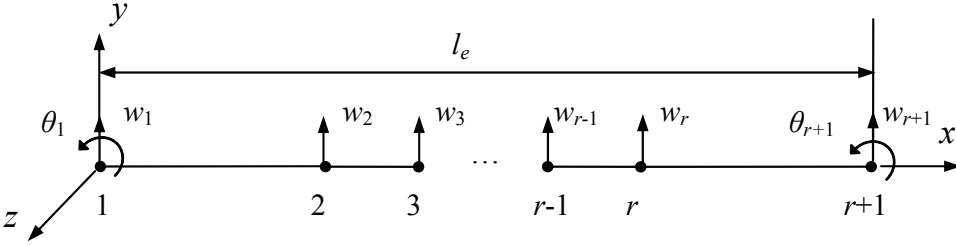
Figure 3: Layout of elemental nodes and the corresponding degree of freedom.

The element is abbreviated to BSWI mj Rayleigh–Euler beam element. Then elemental displacement and slope can be represented by

$$\mathbf{w}^e = \{w_1 \theta_1 w_2 w_3 \cdots w_r w_{r+1} \theta_{r+1}\}^T \tag{5}$$

Where $\theta_1 = \frac{1}{l_e}\frac{dw_1}{d\xi}$ and $\theta_{r+1} = \frac{1}{l_e}\frac{dw_{r+1}}{d\xi}$ denote rotation on each elemental endpoint. The unknown field function $w(\xi,t)$ can be expressed as

$$w(\xi,t) = \mathbf{\Phi} mathbf T_b^e \mathbf{w}^e \tag{6}$$

Where $\mathbf{\Phi} = \left\{\phi_{m,-m+1}^j(\xi)\ \phi_{m,-m+2}^j(\xi)\ldots\phi_{m,2^j-1}^j(\xi)\right\}$ is the column vector combined by the BSWI scaling functions for order m at the scale j (the explicit expression of the functions can be seen in [Dong, Chen, Li, Qi and He (2009)]), and the C_1 type transformation matrix T_b^e is given by

$$\mathbf{T}_b^e = ([\mathbf{\Phi}(\xi_1)\frac{1}{l_e}\frac{d\mathbf{\Phi}(\xi_1)}{d\xi}\mathbf{\Phi}(\xi_2)\ldots\mathbf{\Phi}(\xi_r)\mathbf{\Phi}(\xi_{r+1})\frac{1}{l_e}\frac{d\mathbf{\Phi}(\xi_{r+1})}{d\xi}]^T)^{-1} \tag{7}$$

Substituting displacement function Eq. (6) into Eqs. (3) and (4), respectively, we can obtain

$$\begin{cases} U^e &= \frac{1}{2}(\mathbf{w}^e)^T \mathbf{K}_b^e(\mathbf{w}^e) \\ T^e &= \frac{1}{2}\left(\frac{\partial \mathbf{w}^e}{\partial t}\right)^T \mathbf{M}_b^e\left(\frac{\partial \mathbf{w}^e}{\partial t}\right) + \frac{1}{2}\left(\frac{\partial \mathbf{w}^e}{\partial t}\right)^T \mathbf{M}_r^e\left(\frac{\partial \mathbf{w}^e}{\partial t}\right) \end{cases} \tag{8}$$

Where $\mathbf{K}_b^e$, $\mathbf{M}_b^e$, $\mathbf{M}_r^e$ are the bending stiffness matrixes, translational mass matrix and rotatory inertia mass matrix of the structure respectively, their explicit expression of the functions can be seen in [Dong, Chen, Li, Qi and He (2009)].

The elemental Lagrangian function L_a is

$$L_a = U^e - T^e = \frac{1}{2}(\mathbf{w}^e)^T \mathbf{K}_b^e (\mathbf{w}^e) - \frac{1}{2}(\frac{\partial \mathbf{w}^e}{\partial t})^T \mathbf{M}_b^e (\frac{\partial \mathbf{w}^e}{\partial t}) - \frac{1}{2}(\frac{\partial \mathbf{w}^e}{\partial t})^T \mathbf{M}_r^e (\frac{\partial \mathbf{w}^e}{\partial t}) \quad (9)$$

Applying Hamilton's principle to the elemental Lagrangian function L_a, we can obtain the elemental free vibration equation

$$(\mathbf{M}_b^e + \mathbf{M}_r^e)(\frac{\partial^2 \mathbf{w}^e}{\partial t^2}) + \mathbf{K}_b^e \mathbf{w}^e = 0 \tag{10}$$

and the corresponding elemental free vibration frequency equations is

$$\left| \mathbf{K}_b^e - \omega_n^2 (\mathbf{M}_b^e + \mathbf{M}_r^e) \right| = 0 \tag{11}$$

Where ω_n is the natural frequency.

A transverse crack of depth b is considered on a shaft of diameter d (the corresponding radius is R) as shown in Fig. 4. The crack introduces a local flexibility that is a function of crack depth, and the flexibility changes the stiffness of rotor. Suppose the crack is located between wavelet-based elements and the numbers of two nodes are j and $j+1$ respectively (See Fig. 5). The continuity condition at crack position indicates that the left node and right node have the same vertical deflection, $w_j = w_{j+1}$, while their rotations θ_j and θ_{j+1} are connected through the stiffness matrix $\mathbf{K}_s$ [Dimarogonas and Papadopoulos (1983)]

$$\mathbf{K}_s = \begin{bmatrix} k_t & -k_t \\ -k_t & k_t \end{bmatrix} \tag{12}$$

$$k_t = \frac{\pi E R^8}{32(1-\mu)} \times \frac{1}{\int_{-\sqrt{R^2-(R-b)^2}}^{\sqrt{R^2-(R-b)^2}} (R^2-b^2)[\int_0^{a(\xi)} \eta F^2(\eta/H) d\eta] d\xi} \tag{13}$$

Where k_t is the local stiffness due to the crack, μ is the Poisson's ratio, $a(\xi) = \sqrt{R^2-\xi^2} - R + b$, $H = 2\sqrt{R^2-\xi^2}$ and the function $F(\eta/H)$ can be given by the experimental formula [Tada, Paris and Irwin (2000)].

$$F(\eta/H) = 1.122 - 1.40(\eta/H) + 7.33(\eta/H)^2 - 13.08(\eta/H)^3 + 14.0(\eta/H)^4 \tag{14}$$

Eq. (13) is a function of normalized crack size only and can be computed by numerical integration.

Hence, we can assemble cracked stiffness submatrix $\mathbf{K}_s$ into the global stiffness matrix easily. The position of $\mathbf{K}_s$ in the global stiffness matrix is determined by crack location a. The global mass matrix of cracked rotor system is equal to the uncracked one. From now on, the cracked rotor system finite element model is constructed by using BSWI beam element. The solution of the eigenvalue problem can then proceed as usual.
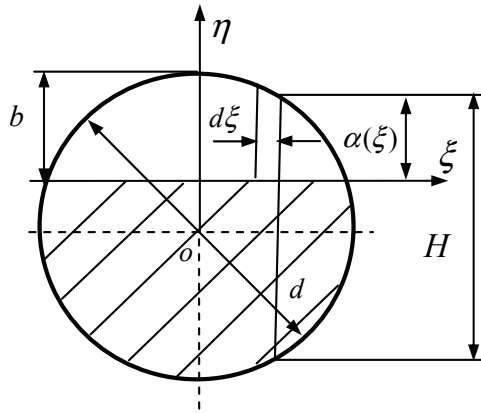
Figure 4: Geometry of a cracked section in rotor.
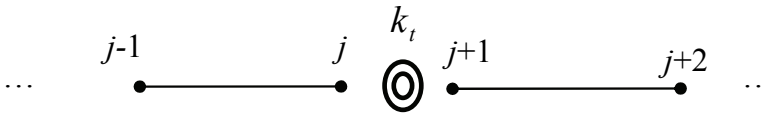
Figure 5: Layout of the corresponding nodes around crack with stiffness coefficient k_t.

2.3 Inverse problem: multiple crack identification

2.3.1 Damage coefficient method

According to Castigliano's theorem, the local displacement $\bar{u}$ due to the crack can be expressed as

$$\bar{u} = \frac{\partial \bar{W}}{\partial p} \tag{15}$$

Where $\bar{W}$ is local strain energy due to crack, p is the force or moment of structure, as shown in Fig. 6. For crack element, $\bar{W} = \int_0^b J(\alpha)d\alpha$, α is crack normalized depth, $\alpha = b/d$, and $J(\alpha)$ is energy density function.
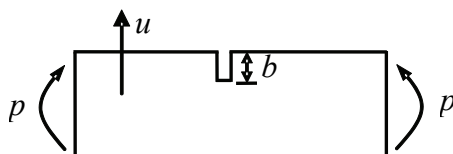
Figure 6: Crack element

The local flexibility c due to the crack can be defined as

$$c = \frac{\partial \bar{\mu}}{\partial p} \tag{16}$$

and the local stiffness k_t due to the crack is $k_t=1/c$, we put Eq. (15) into Eq. (16), and obtain

$$\frac{1}{k_t} = \frac{\partial^2 \bar{W}}{\partial p^2} \tag{17}$$

It is an effective method to treat the crack as a rotating spring model. When the structure is intact, the spring stiffness k_t is infinite. k_t increases as the crack depth enlarges. Gudmundson given the relation of natural frequencies between the damage structures and intact ones [Gudmudson (1982)]:

$$\frac{\bar{\omega}_n^2}{\omega_n^2} = 1 - \frac{\bar{W}_n}{W_n} \tag{18}$$

Where, $\bar{\omega}_n$ and ω_n are the natural frequencies for damage structure and intact one respectively. $\bar{W}_n$ is n the order strain energy due to crack, W_n is strain energy for the n order model of intact structure.

According to Eq. (18), we have $\frac{\omega_n^2 - \bar{\omega}_n^2}{\omega_n^2} = \frac{\bar{W}_n}{W_n} \Rightarrow \frac{(\omega_n + \bar{\omega}_n)(\omega_n - \bar{\omega}_n)}{\omega_n^2} = \frac{\bar{W}_n}{W_n}$. Because $(\omega_n + \bar{\omega}_n) \approx 2\omega_n$, so the Eq. (18) can be written as

$$\frac{\Delta \omega_n}{\omega_n} = \frac{1}{2} \cdot \frac{\bar{W}_n}{W_n} \tag{19}$$

Where $\Delta \omega_n = \omega_n - \bar{\omega}_n$. By integral transformation, the Eq. (17) is

$$\bar{W}_n = \frac{p_n^2}{2k_t} \tag{20}$$

Where p_n is the inner force of structure for the n order model. When the pure bending vibration is considered, p_n^2 is direct proportion with the n order strain energy density function $\bar{\Psi}_n$, $\bar{\Psi}_n = p_n^2/2EI_z$. So the Eq. (20) can be written:

$$\bar{W}_n = \frac{\bar{\Psi}_n(\beta) \cdot EI_z}{k_t} \tag{21}$$

Where β is crack normalized location. For the intact structure, W_n can be obtained through integral transformation for $\Psi_n(\beta)$,

$$W_n = L \int_0^1 \Psi_n(\beta)\mathrm{d}\beta \tag{22}$$

Because the crack has little effectiveness for modal shape of structure, the energy density function of damage structure $\bar{\Psi}_n$ is same as intact one Ψ_n. Combining Eqs. (19), (21) and (22), we can obtain,

$$\frac{\Delta\omega_n}{\omega_n} = 2g_n(\beta)\frac{1}{K} \tag{23}$$

Where,

$$g_n(\beta) = \frac{\Psi_n(\beta)}{4\int_0^1 \Psi_n(\beta)\mathrm{d}\beta} \tag{24}$$

where $K = \frac{k_t L}{EI_z}$, K indicts the depth of crack. The strain energy density function for the n order model of intact structure is

$$\Psi_n(\beta) = E(\beta)I(\beta)\left[\phi_n''(\beta)\right]^2 \tag{25}$$

Where $\phi_n''(\beta)$ is second derivative of n order model shape. For the structure with multiple crack, we expand Eq. (23), and obtain

$$\frac{\Delta\boldsymbol{\omega_n}}{\boldsymbol{\omega_n}} = 2\sum_{i=1}^m g_n(\beta_i)\cdot\frac{1}{k_i} \tag{26}$$

Where β_i is the normalized crack location of the i crack, and the m is crack number.

In the damage mechanics theory, the damage caused by crack can be calibrated by damage coefficient **S**. And if the coefficient of the unit is greater than zero, this unit would be diagnosed as a cracked unit and the magnitude of the coefficient reflected

the crack depth. Hu and Liang [Hu and Liang (1993)] introduced the theory into multiple crack identification, and obtained:

$$\frac{\Delta\omega_n}{\omega_n} = 2\sum_{i=1}^{m} \int_{e_i} \frac{\frac{\Psi[\phi_n(\beta)]}{4\int_v \Psi[\phi_n(\beta)]}}{} \, dV \cdot s_i \tag{27}$$

Where e_i stands for the i element solve domain. The Eq. (26) can be written as

$$\frac{\Delta\boldsymbol{\omega_n}}{\boldsymbol{\omega_n}} = 2\sum_{i=1}^{m} \int_{e_i}^{g_n(\beta)} d\beta \cdot s_i \tag{28}$$

In practice, we divide the shaft into m elements. If the n order model of shaft is known, the Eq. (28) can be expanded as

$$\frac{\Delta\boldsymbol{\omega}}{\boldsymbol{\omega}}_{n\times 1} = 2\mathbf{H}_{n\times m} \cdot \mathbf{S}_{m\times 1} \tag{29}$$

Where, the matrix $\mathbf{H}$ includes the element $h_{ij} = \int_{e_i}^{g_i(\beta)} d\beta$.

2.3.2 WFEM based multiple crack identification method

To identify the structural multiple cracks parameters accurately and efficiently; we meshed different regions with the WFEM, and proposed an algorithm for the identification of multiple cracks in rotor. And we have the block diagram of the algorithm shown in Fig.7, the identification procedure is as following:

- By practical measurement, we can obtain the change rate of natural frequency $\Delta\boldsymbol{\omega}/\boldsymbol{\omega}$. Then divide the entire structure into m wavelet finite elements;

- Input structural material and geometry parameters, we can calculate the influence matrix $\mathbf{H}$ with integral operation;

- Substitute matrix $\Delta\boldsymbol{\omega}/\boldsymbol{\omega}$ and $\mathbf{H}$ into Eq. (29), obtain the damage influential matrix $\mathbf{S}$. Moreover, the number of non-zero elements in matrix $\mathbf{S}$ represents the number of the predicted cracks. Corresponding to the non-zero elements is the damaged unit containing cracks. A positive value s_j is to represent the decrease of the section modulus. Conversely, a negative value s_j means the increase of the section modulus. However, it is impossible for the section modulus to increase. Therefore, we consider the unit represented by $s_j<0$ is in good condition. That is, we set s_j to zero and re-calculate the damage influential matrix till only the non-negative values are included in matrix $\mathbf{S}$. The number of elements contained in matrix $\mathbf{S}$ is corresponding to the number of cracks, and the element position reflects the region of the structural crack;

- To detect the depth of the crack, we need to calculate the change rate of the first three orders of natural frequency corresponding by the damage coefficient in each cracked element;

- We take the change rate as input parameter of the three-line intersection in a single crack detection method [Li, Chen and He (2005)] and plot the frequency contour line of each mode. The intersection of the three contour lines predicts the specific position and depth of the crack.

3 Example verification

The validity of the proposed method is testified by a simulation of rotor system with two cracks, as shown in Fig. 8. Dimensions of the rotor are total length $L = 300$mm, diameter $d = 10$mm. The corresponding material properties are: $E = 2.06e11$N / m^2, $\rho = 7860$kg / m^3 and $\mu = 0.3$. The positional dimensions of the two cracks are: a_1 and a_2, relative position β_1 and β_2 are defined as: $\beta_1 = a_1/L$ and $\beta_2 = a_2/L$.

30 BSWI Rayleigh-Timoshenko beam elements are used to discrete the rotor. The model database of crack diagnosis forward problem is established according to the different location and depth of crack, as shown in Fig. 9. Fig. 10 shows how first three natural frequency rate changes with different depths of the two cracks at different locations.

As can be seen from Fig. 10 (a), when β_1 and β_2 get close to 1/2, crack depth has the most obvious influence on the first natural frequency of rotor. From Fig. 10 (b), crack depth has the most significant influence on the second natural frequency of rotor when β_1 and β_2 get close to 1/4. Similar to the above, in Fig. 10 (c), when β_1 and β_2 get close to 1/6, crack depth has the most obvious influence on the third natural frequency of rotor.

According to Euler beam theory, i order modal shape of the simply supported rotor shown in Fig. 8 is

$$\phi_i(\beta) = \sin(i\pi\beta) \tag{30}$$

Where $\beta = x/L \in [0,1]$, x is showed in Fig. 8. From Eq. 24:

$$g_i(\beta) = \frac{1}{4} \frac{[\phi_i''(\beta)]^2}{\int_0^1 [\phi_i''(\beta)]^2 d\beta} = \frac{1}{2} \sin^2(i\pi\beta) \tag{31}$$

Then the element h_{ij} of influence matrix **H** is:

$$h_{ij} = \int_{e_i} g_i(\beta) d\beta = \frac{1}{2} \cdot \int_{e_i} \sin^2(i\pi\beta) d\beta \tag{32}$$

Start

Input $\Delta\omega_n, \omega_n$ $(n = 1,2,3,\ldots)$

Divide the beam into m elements

Input material and geometric parameters,

Calculate h_{ij}

Form the equation $\Delta\omega_n/\omega_n = 2\mathbf{HS}$

Solve $\Delta\omega_n/\omega_n = 2\mathbf{HS}$ for $\mathbf{S}$

Set negative s_j to zero

No

All $s_j \geq 0$

Yes

Crack number and region

Crack element

Solve s_j to obtain $\Delta\omega_r/\omega_r$

In element j, input $\Delta\omega_n/\omega_n$ into contour method, and solve α and β

Output α and β

End
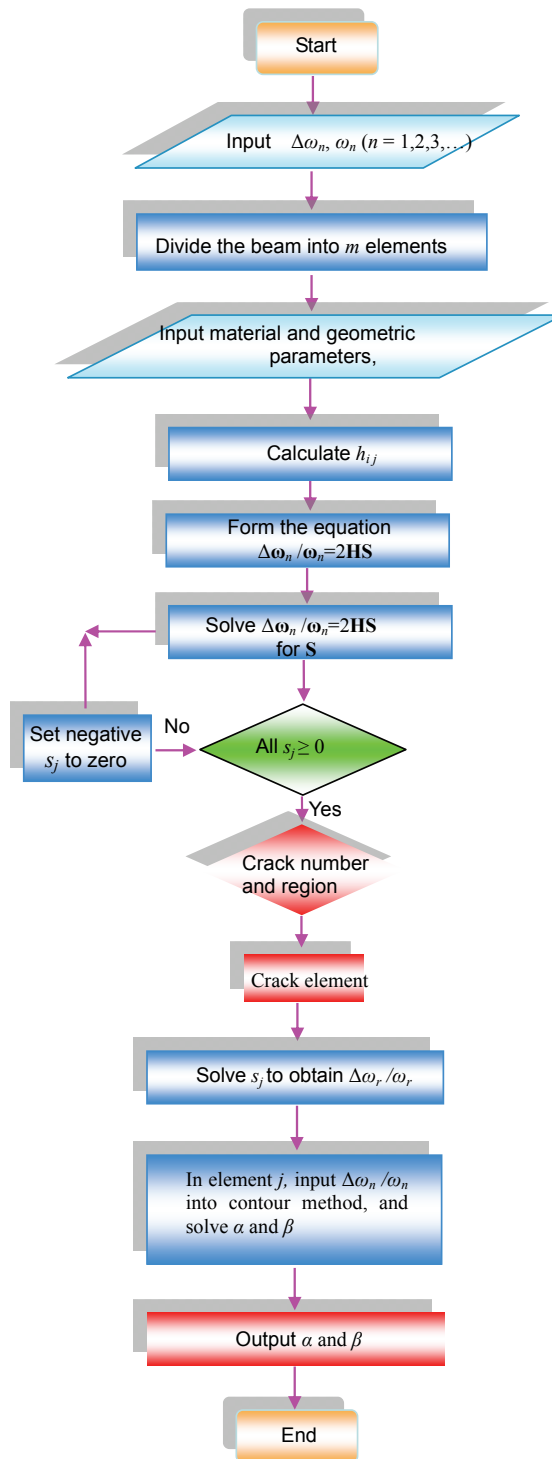
Figure 7: The block of algorithm for multiple cracks in rotor using WFEM
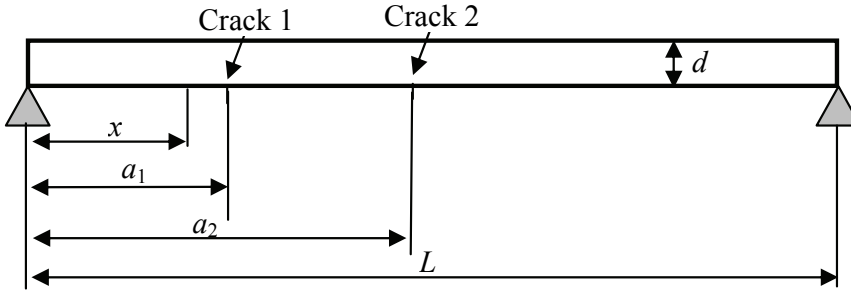
Figure 8: A rotor with two cracks

(i=1,2, …, n, j =1,2, …, m)

The first three function $g_i(\beta)(i = 1,2,3)$ of the simply supported rotor is shown in Fig. 11.

Based on the assumption that the first five natural frequencies of the two-crack rotor are known, when the rotor is divided into 10 elements, h_{ij} could be calculated by Eq. 32; the results are shown in Tab.1.

Table 1: The index h_{ij}(n=5, m=10) for simple supported rotor

i \ j	1	2	3	4	5	6	7	8	9	10
1	0.0016128	0.010546	0.025	0.039454	0.048387	0.048387	0.039454	0.025	0.010546	0.0016128
2	0.0060793	0.032227	0.048387	0.032227	0.0060793	0.0060793	0.032227	0.048387	0.032227	0.0060793
3	0.012386	0.04541	0.025	0.0045905	0.037614	0.037614	0.0045905	0.025	0.04541	0.012386
4	0.019153	0.040307	0.0060793	0.040307	0.019153	0.019153	0.040307	0.0060793	0.040307	0.019153
5	0.025	0.025	0.025	0.025	0.025	0.025	0.025	0.025	0.025	0.025

Then we verify the precision and reliability of BSWI finite element model used in quantitative diagnosis of multi-crack rotor. We still use 900 Rayleigh-Timoshenko Beam Elements to solve natural frequencies of the cracked rotor under different working conditions, and the obtained natural frequencies are regarded as "testing" frequencies (crack conditions and their corresponding frequencies are shown in Tab.2). By substitution of the "testing" frequencies into Eq. 29, the inverse problem is solved. Because of the symmetric structure, we assume that two cracks are both located in the left part of rotor.

The two-crack rotor shown in Fig. 8 is divided into 10 elements of same length.
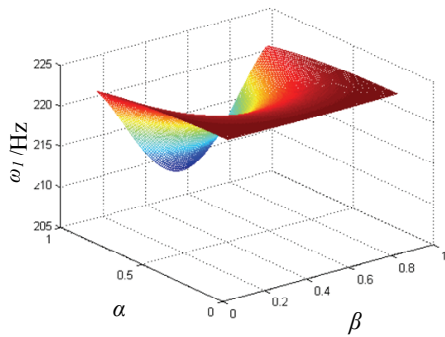
(a) Natural frequency of the first order
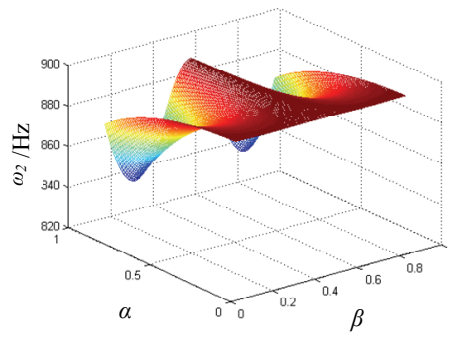
(b) Natural frequency of the second order
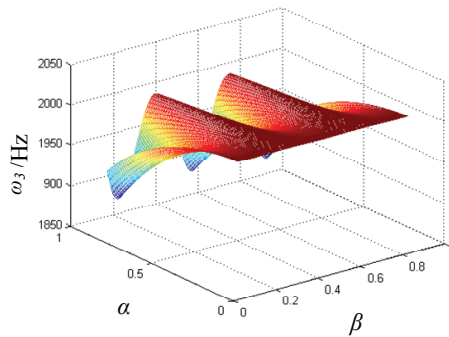
(c) Natural frequency of the third order

Figure 9: The relation between frequency $\omega_n(n=1, 2, 3)$ and crack normalized location β ($\beta = a/L$),normalized depth α ($\alpha = b/d$)

Table 2: The cases for two crack rotor

Case	β_1	α_1	β_2	α_2	Result of 900 traditional elements				
					ω_1 /Hz	ω_2 /Hz	ω_3 /Hz	ω_4 /Hz	ω_5 /Hz
0			Intact rotor		223.301	892.294	2004.295	3554.986	5538.641
I	0.35	0.5	0.45	0.5	217.537	882.688	1980.867	3492.084	5461.624
II	0.25	0.4	0.35	0.4	220.794	879.641	1995.396	3527.633	5491.750

(a) Natural frequency variance ratio of the first order

(b) Natural frequency variance ratio of the second order

(c) Natural frequency variance ratio of the third order
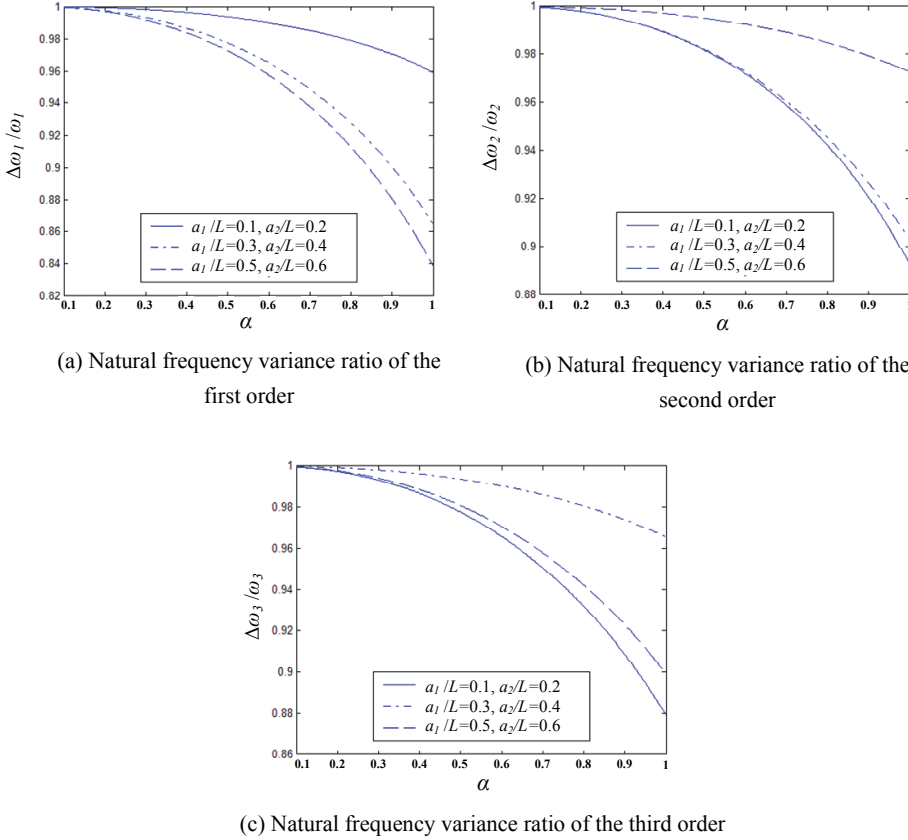
Figure 10: Variance rations for the first three order natural frequencies

In case ¢ñ, two cracks are separately located in the fourth and fifth element. We substituted the coefficient h_{ij} and the first five frequencies into Eq. 29 and we get the equation:

$$\frac{\Delta\boldsymbol{\omega}}{\boldsymbol{\omega}}\bigg|_{5\times 1} = 2\mathbf{H}_{5\times 10}\cdot\mathbf{S}_{10\times 1} \tag{33}$$

Damage coefficients ($\{s_1,s_2,\ldots,s_{10}\}^T$) are obtained by solving the equation above.

$$\begin{aligned}
\mathbf{S} &= \{s_1,s_2,s_3,s_4,s_5,s_6,s_7,s_8,s_9,s_{10}\}^T \\
&= \{-0.0074962, 0.0015769, -0.0056386, 0.078146, 0.072466, 0, 0, 0, 0, 0\}^T
\end{aligned} \tag{34}$$
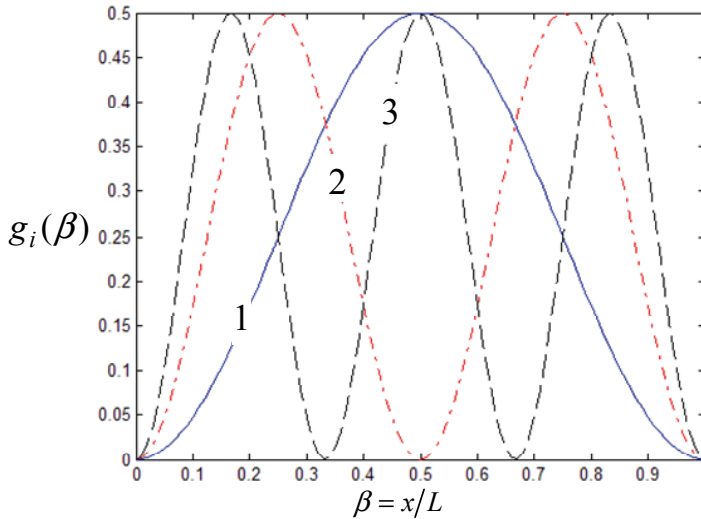
Figure 11: Simple supported rotor $g_i(\beta)$ (1: The first order; 2: The second order; 3: The third order)

Because the structure is symmetric, only the left part should be taken into consideration. As a result, $s_6, s_7, \ldots, s_{10}$ are set zero. Damage coefficients s_1 and s_3 are less than zero which means that the stiffness of Element 1 and Element 3 increase, which is not correspondent with practice. So s_1 and s_3 are also set zero, which means there is no crack in Element 1 and Element 3. After recalculating Eq. 33, the newest damage coefficients are obtained.

$$\mathbf{S} = \{s_2, s_4, s_5\}^T = \{-0.0064824, 0.15125, 0.14404\}^T \tag{35}$$

Because s_2 is less than zero, it is set zero. Repeat the process above, we got the final $\mathbf{S}$:

$$\mathbf{S} = \{s_4, s_5\}^T = \{0.14812, 0.14128\}^T \tag{36}$$

All elements in damage coefficients matrix are nonnegative, we could predict that Element 4 and Element 5 are crack elements, which agrees with case ¢ñ.

By substitution of s_4 into Eq. 33 and other damage coefficients set zero, we get natural frequency change rate of cracked rotor caused by the crack in Element 4, $\Delta\omega_1/\omega_1 = 1.1688\%$, $\Delta\omega_2/\omega_2 = 0.9547\%$, $\Delta\omega_3/\omega_3 = 0.1360\%$, then with the first three natural frequencies and single crack quantitative diagnosis database (shown

(a) Frequency contour for crack 1 (b) Frequency contour for crack 2
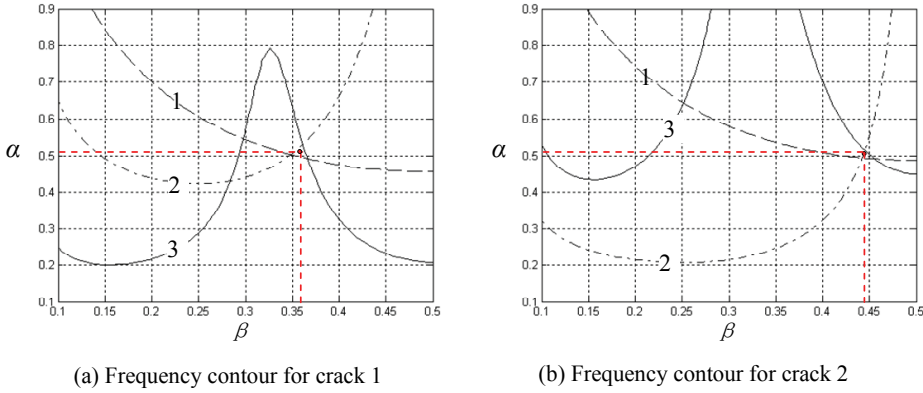
Figure 12: Frequency contours for case I ($m = 10$) (1: The first order frequency contour; 2: The second order frequency contour; 3: The third order frequency contour)

in Fig. 9), we use contour method to diagnose cracks. Contour lines of frequency are shown in Fig. 12. Diagnosis results are listed in Tab. 3.

Table 3: Prediction results for case ¢ñ ($m=10$)

Cases	β_1	α_1	β_1^*	α_1^*	β_2	α_2	β_2^*	α_2^*
			（Error）	（Error）			（Error）	（Error）
I	0.35	0.5	0.36 (1%)	0.51 (1%)	0.45	0.5	0.445 (0.5%)	0.51 (1%)

* The predicted results.

Identification accuracy of multiple cracks is not very ideal (maximum error being 1%), it is mainly because that element number (m=10) of the rotor is not enough. In order to improve identification accuracy, the rotor is divided into 30 elements. In case ¢ñ, two cracks are separately located in the eleventh and fourteenth element. The identification process is the same as the process above. The final damage coefficient matrix is:

$$\mathbf{S} = \{s_{11}, s_{13}, s_{14}\}^T$$
$$= \{0.41752, 0.026592, 0.41901\}^T$$

(37)

Obviously, Element 11, 13, 14 are cracked elements. The first three natural frequency change rates of cracked rotor caused by the crack in Element 13 are $\Delta\omega_1/\omega_1 = 0.0772\%$, $\Delta\omega_2/\omega_2 = 0.0397\%$, $\Delta\omega_3/\omega_3 = 0.0187\%$. The frequency change rates are very small, which can be neglected. Actually there is no crack in this element.

We use contour method to diagnose cracks. Frequency contour lines are shown in Fig. 13. The diagnosis results of the cracks separately located in Element 11 and Element 14 are listed in Tab 4.

In case I, the frequency contour lines are shown in Fig. 14. Diagnosis results are listed in Tab. 5.

From Tab.4 and Tab. 5 we can conclude that high identification accuracy of multiple cracks has been achieved using BSWI finite element model. The maximum relative error of crack location identification is 0.6%, while the maximum relative error of crack location identification is 0.7%. So the precision and reliability of this method has been verified.

Table 4: Prediction results for case I (m=30)

Case	β_1	α_1	β_1^* (Error)	α_1^* (Error)	β_2	α_2	β_2^* (Error)	α_2^* (Error)
I	0.35	0.5	0.349 (0.1%)	0.493 (0.7%)	0.45	0.5	0.452 (0.2%)	0.498 (0.2%)

* The predicted results.

Table 5: Prediction results for case II (m=30)

Case	β_1	α_1	β_1^* (Error)	α_1^* (Error)	β_2	α_2	β_2^* (Error)	α_2^* (Error)
II	0.25	0.4	0.244 (0.6%)	0.404 (0.4%)	0.35	0.4	0.353 (0.3%)	0.402 (0.2%)

* The predicted results.

(a) crack 1

(b) crack 2

(c) Zoom in of frequency contour for crack 1

(d) Zoom in of frequency contour for crack 2
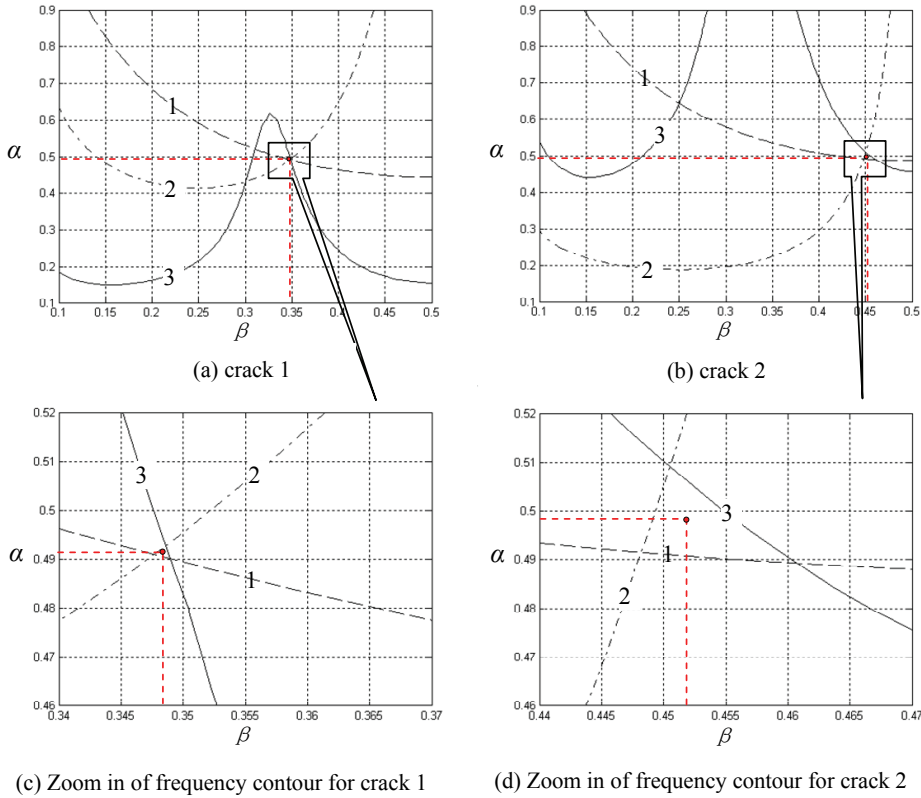
Figure 13: Frequency contours for case I ($m = 30$) (1: The first order frequency contour; 2: The second order frequency contour; 3: The third order frequency contour)

4 Conclusions

The changes of structural natural frequency caused by multiple cracks are consistent with the linear superposition relation. That is, the changes of natural frequency caused by multiple cracks are equivalent to the sum of that caused by single crack under the same working conditions. As a result, each damage coefficient is corresponding to each crack. In this paper, a novel method of multiple cracks rotor identification based on WFEM was proposed. The key to successful impletion of multiple cracks quantitative diagnosis in the engineering practice was addressed:

(a) crack 1   (b) crack 2
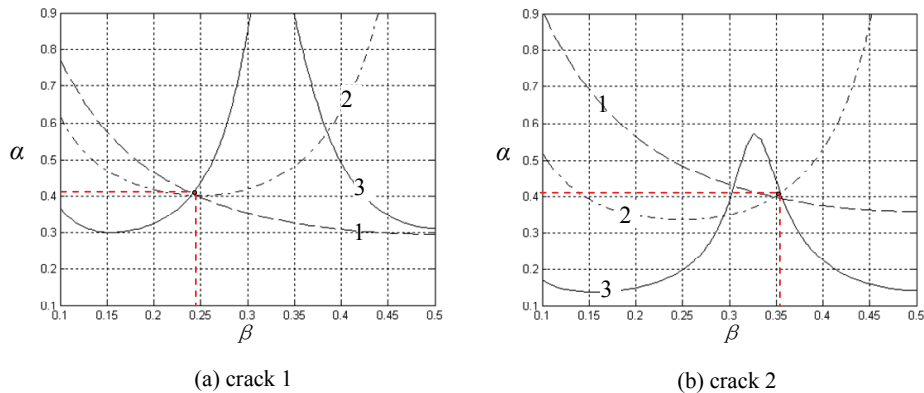
Figure 14: Frequency contours for case II ($m = 30$) (1: The first order frequency contour; 2: The second order frequency contour; 3: The third order frequency contour)

1. Establishing an accurate and reasonable finite element structural modal to make the calculated values of natural frequency agree well with the measured values;

2. Firstly determine the number of the structural cracks, then perform quantitative diagnosis on each crack.

References

Anjan, D; Talukdar, S. (2004): Damage detection in bridges using accurate modal parameters. *Finite El. A.*, vol. 40, pp. 287–304.

Bao, Y. G; Wang, X. D. (2011): Identification of multiple cracks based on optimization methods using harmonic elastic waves. *Int. J. Fract.*, vol. 172, pp. 77-95.

Chen, X. F; Li, B; Zi, Y. Y; He, Z. J. (2005): Multiple infant cracks detection for beam-type structures by wavelet finite element method. *Chin. J. Mech. Eng. (Engl. Ed.)*, vol. 7, pp. 126-129.

Dimarogonas, A. D. (1996): Vibration of cracked structures: a state of the art review. *Eng. Fract. M.*, vol. 55, pp. 831-857.

Dimarogonas, A. D.; Papadopoulos, C. A. (1983): Vibration of cracked shafts in

bending. *J. Sound. Vib.*, vol. 91, pp. 583–893.

Dong, H. B; Chen, X. F.; Li, B; Qi, K. Y.; He, Z. J. (2009): Rotor crack detection based on high-precision modal parameter identification method and wavelet finite element model. *Mech. Syst. S.*, vol. 23, pp. 869-883.

Gasch, R. (1993): A survey of the dynamic behavior of a simple rotating shaft with a transverse crack. *J. Sound. Vib.*, vol. 160, pp. 313-332.

Goswami, J. C; Chan, A. K; Chui, C. K. (1995): On solving first-kind integral equations using wavelets on a bounded interval. *IEEE Antenn.*, vol. 43, pp. 614-622.

Green, I.; Casey, C. (2005): Crack detection in a rotor dynamic system by vibration monitoring-Part I: analysis. *J. Eng. Gas. T.*, vol. 127, pp. 425-436.

Gudmudson, P. (1982): Eigen frequency changes of structures due to crack, notches or other geometrical changes. *J. Mech. Phys.solids*, vol. 30, pp. 339-352.

He, Z. Y; Lu, Z. R. (2010): Time domain identification of multiple cracks in beam. *Struc. Eng. M.*, vol. 35, pp. 773-789.

Hollander, D; Wunsche, M; Henkel, S; Theilig, H. (2012): Numerical simulation of multiple fatigue crack growth with additional crack initiation. *Key Eng. Mat.*, vol. 488-489, pp. 444-447.

Hu, J. L; Liang, R. (1993): An integrated approach to detection of cracks using vibration characteristics. *J. Franklin I.*, vol. 330, pp. 841-853.

Kardestuncer, H.; Norrie, D. H. (1987): Finite Element Handbook, McGraw-Hill Book Company, New York.

Lam, H. F; Yin, T. (2010): Statistical detection of multiple cracks on thin plates utilizing dynamic response. *Eng. Struct.*, vol. 32, pp. 3145-3152.

Lee J. (2009): Identification of multiple cracks in a beam using vibration amplitudes. *J. Sound. Vib.*, vol. 326, pp. 205-212.

Lele, S. P.; Maiti, S. K. (2002): Modeling of transverse vibration of short beams for crack detection and measurement of crack extension. *J. Sound. Vib.*, vol. 257: pp. 559–583.

Li, B; Chen, X. F.; He, Z. J. (2005): Detection of Crack Location and Size in Structures Using Wavelet Finite Element Methods. *J. Sound. Vib.*, vol. 285, pp. 767-782.

Li, B; Dong H. B; Xiang J. W.; Qi, K. Y.; He, Z. J. (2011): Vibration Based Crack Identification of Running Rotor System. *Adv. Sci. Lett.*, vol. 4, pp. 1638-1642.

Liang, R. Y; Hu, J. L; Choy, F. (1992): Quantitative NDE technique for assessing damages in beam structures. *J. Eng. Mec.*, vol. 118, pp. 1468-1487.

Lin, R. J; Cheng, F. P. (2008): Multiple crack identification of a free-free beam with uniform material property variation and varied noised frequency. *Eng. Struct.*, vol. 30, pp. 909-929.

Morassi, A. (2001): Identification of a crack in a rod based on changes in a pair of natural frequencies. *J. Sound. Vib.*, vol. 242: pp. 577–596.

Naniwadekar, M. R.; Naik, S. S.; Maiti, S. K. (2008): On prediction of crack in different orientations in pipe using frequency based approach. *Mech. Syst. S.*, vol. 22, pp. 693–708.

Patil, D. P.; Maiti, S. K. (2003): Detection of multiple cracks using frequency measurements. *Eng. Fract. M.*, vol. 701, pp. 553-1572.

Ruotolo, R; Surace, C. (2004): Natural frequencies of a bar with multiple cracks. *J. Sound. Vib.*, vol. 272, pp. 301-316.

Salawu, O. S. (1997): Detection of structural damage through changes in frequency: a review. *Eng. Struct.*, vol. 19, pp. 718-723.

Sekhar, A. S. (2004): Crack identification in a rotor system: a model-based approach. *J. Sound. Vib.*, vol. 270, pp. 887–920.

Sekhar, A. S. (2008): Multiple cracks effects and identification. *Mech. Syst. S.*, vol. 22, pp. 845-878.

Sekhar, A. S. (2011), Some recent studies on cracked rotors. In: K. Gupta (ed) *IUTAM symposium on emerging trends in rotor dynamics*, Springer, London, pp. 491-503.

Tada, H.; Paris, P. C.; Irwin, G. R. (2000): The Stress Analysis of Cracks Handbook, ASME Press, New York.

Xiang, J. W.; Liang, M. (2011): Multiple crack identification using frequency measurement. *World Acad. Sci. Eng. Technol.*, vol. 76, pp. 311-316.

Xiang, J W; Zhong, Y. T.; Chen, X. F.; He, Z. J. (2008): Crack detection in a shaft by combination of wavelet-based elements and genetic algorithm. *Int. J. Sol. S.*, vol. 45, pp. 4782-4795.

Zhang, X. Q; Han, Q; Li, F. (2010): Analytical approach for detection of multiple cracks in a beam. *J. Eng. Mec.*, vol. 136, pp. 345-357.